

Damage prediction for magnesium matrix composites formed by liquid-solid extrusion process based on finite element simulation

QI Le-hua(齐乐华)^{1,2}, LIU Jian(刘 健)¹, GUAN Jun-tao(关俊涛)¹,
SU Li-zheng(苏力争)¹, ZHOU Ji-ming(周计明)^{1,2}

1. School of Mechatronic Engineering, Northwestern Polytechnical University, Xi'an 710072, China;

2. Key Laboratory of Contemporary Design and integrated Manufacturing Technology, Ministry of Education, Northwestern Polytechnical University, Xi'an 710072, China

Received 13 May 2010; accepted 25 June 2010

Abstract: A damage prediction method based on FE simulation was proposed to predict the occurrence of hot shortness cracks and surface cracks in liquid-solid extrusion process. This method integrated the critical temperature criterion and Cockcroft & Latham ductile damage model, which were used to predict the initiation of hot shortness cracks and surface cracks of products, respectively. A coupling simulation of deformation with heat transfer as well as ductile damage was carried out to investigate the effect of extrusion temperature and extrusion speed on the damage behavior of $C_{sf}/AZ91D$ composites. It is concluded that the semisolid zone moves gradually toward deformation zone with the punch descending. The amplitude of the temperature rise at the exit of die from the initial billet temperature increases with the increase of extrusion speed during steady-state extrusion at a given punch displacement. In order to prevent the surface temperature of products beyond the incipient melting temperature of composites, the critical extrusion speed is decreased with the increase of extrusion temperature, otherwise the hot shortness cracks will occur. The maximum damage values increase with increasing extrusion speed or extrusion temperature. Theoretical results obtained by the DeformTM-2D simulation agree well with the experiments.

Key words: magnesium matrix composite; liquid-solid extrusion; hot shortness cracks; surface cracks; finite element method

1 Introduction

Liquid-solid extrusion is a new forming technique that combines the merits of liquid metal infiltration and semisolid extrusion. The major advantages of this process are elimination of porosity and shrinkage, good surface finish, good dimensional accuracy, high specific strength and near net shaping[1]. The key technology is to ensure that the billet at the exit of forming die has been solidified during extrusion by adjusting extrusion speed and the solidification rate of semisolid material. Inappropriate process parameters may induce various product defects. Experiments have revealed that the typical product defects are hot shortness cracks and surface cracks. The finite element method (FEM) can play an important role in understanding the mechanism of these product defects by analyzing the process variables that are not experimentally measurable. Defects caused by extrusion speed and temperature during hot

extrusion were analyzed by use of finite element simulation, and the forming limit diagrams of aluminum alloy, magnesium alloy and their composites were established[2–6]. The influence of process parameters and die structure on the surface damage of composite was simulated with ductile fracture criteria[7–10]. WANG et al[11] qualitatively analyzed the mechanism of forming defects in the process of liquid-solid extrusion by use of 3D coupled thermo-mechanical finite element simulation. However, for the simulation of forming magnesium matrix composite in semisolid state, there is a scarcity of information available in the open literature. In the present work, the finite element model which characterized the heat conduction and damage evolution in the liquid-solid extrusion process for $C_{sf}/AZ91D$ composites was established, and the influence of extrusion speed and extrusion temperature on the damage evolution was analyzed. The occurrence of hot shortness cracks and surface cracks were predicted quantitatively by adopting a novel damage prediction method. Finally,

the simulated results were verified by experiments.

2 Simulation model and scheme

The process of semisolid extrusion was simulated using DEFORMTM-2D finite element modeling software. In view of the axial symmetry of billet, tools, boundary conditions and loads in whole forming process, half of the actual model was selected to establish the FE model in order to reduce the computational workload and storage. The billet and tools were meshed by unique density controlled meshing method. In order to improve the precision and convergence of computation, a maximum interference depth of 0.25 mm was set to trigger the remeshing procedure when the depth that an element edge of billet crosses the surface of forming die exceeded 0.25 mm[12].

To get the thermo-mechanical behavior of the composite during semisolid extrusion, 10% (volume fraction) C_{sf}/AZ91D composite was fabricated by squeeze casting method. The flow stress–strain data of the composite were obtained through hot and semisolid compression tests using Gleeble1500D machine over a temperature range of 323–475 °C and a strain rate range of 0.005–0.5 s⁻¹. Through putting into the material database in the form of data table, DEFORMTM-2D can compute using interpolation method automatically based on these data. The billet is assumed as rigid-viscoplastic material and the die is assumed as rigid body.

It was assumed that hot shortness cracks occurred once the surface temperature (T_b) exceeded the incipient melting temperature (T_s). Thus, the incipient melting temperature can be defined as the criterion for hot shortness cracks. When the deformation temperature of billet is below the incipient melting temperature, the surface cracks of workpiece during extrusion process are generally predicted using Cockcroft & Latham damage model as Eq.(1), which relates to the likelihood of ductile fracture in a part:

$$\int_0^{\bar{\varepsilon}_f} \frac{\sigma_{\max}}{\bar{\sigma}} d\bar{\varepsilon} \geq C \quad (1)$$

where σ_{\max} , $\bar{\sigma}$, $\bar{\varepsilon}$, $\bar{\varepsilon}_f$ and C is the maximum principal stress, equivalent stress, equivalent strain, equivalent fracture strain and critical damage value, respectively.

When damage value is above the critical damage value of the deformation material, surface cracks will occur. The damage distribution is calculated with a weakly-coupled approach without taking into account of its effect on the other thermomechanical fields. And it is achieved by post-processing the finite element analysis for a given load step to calculate the damage distribution using the stress and strain field at this step[13]. Fracture initiation and crack propagation were realized using

element deletion method. In the meantime, remeshing and interpolation were implemented automatically in DEFORM-2D code. As a result, cracks can propagate along accurate direction. In summary, the simulation scheme of the product defects in liquid-solid extrusion is illustrated in Fig.1. The hot shortness cracks and surface cracks are predicted by critical temperature criterion and Cockcroft & Latham damage model, respectively. Finally, the simulated results are compared with experimental ones.

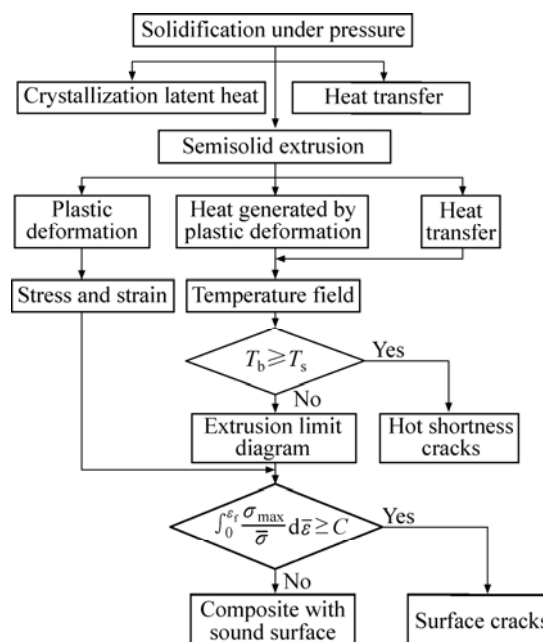


Fig.1 Simulation flowchart of product defects in liquid-solid extrusion

In the process of liquid-solid extrusion, there is a continuous phase transition from liquid state, semisolid state to solid state. The latent heat of crystallization generated during the semisolid forming process has a notable impact on the temperature field. The influence of latent heat is considered using equivalent specific heat method, namely, changing the specific heat of composite in semisolid temperature range[14]:

$$c_{eq} = c_0 + L_f / (T_1 - T_s) \quad (2)$$

where c_{eq} and c_0 are the equivalent specific heat value and original value, respectively; L_f is the crystallization latent heat; T_1 and T_s are the solidus temperature and liquidus temperature of composite, respectively. The thermal physical properties of the composites and tools are listed in Table 1. The solidus and liquidus temperatures of the 10%C_{sf}/AZ91D are 427 °C and 591 °C, respectively.

According to the infiltration–extrusion integrated experiments, parameters adopted in the current finite element simulation are listed in Table 2. Due to the fact

Table 1 Physical properties of composite billet and 3Cr2W8V tools

Material	Temperature/°C	Heat capacity/ (N·mm ⁻² ·°C ⁻¹)	Thermal conductivity/ (W·m ⁻¹ ·°C ⁻¹)	Density/(g·cm ⁻³)	Emissivity
10% C _{sf} /AZ91D	100	1.895	60	1.8	0.12
	427	5.812	65		
	591	6.056	80		
	800	2.400	85		
3Cr2W8V	100	3.909	20.1	8.35	0.7
	200	4.388	22.2		
	500	5.724	24.3		
	800	10.541	23.0		

Table 2 Simulation and experimental parameters

Container insider diameter/mm	Container outsider diameter/mm	Die semi-angle/(°)	Extrusion ratio	Pouring temperature/°C
45	210	55	5	800
Preheating temperature of punch, container, forming die and ejector/°C	Extrusion temperature/°C	Ambient temperature/°C	Extrusion speed/(mm·s ⁻¹)	Punch displacement/mm
200, 650, 550, 550	390–420	20	1–8	35
Friction coefficient between billet and container(punch)	Friction coefficient between billet and forming die	Heat transfer coefficient between billet and environment/ (kW·m ⁻² ·°C ⁻¹)	Heat transfer coefficient between material and tools during solidification/ (kW·m ⁻² ·°C ⁻¹)	Heat transfer coefficient between material and tools during extrusion/ (kW·m ⁻² ·°C ⁻¹)
1	0.3	0.1	1	11

that the billet/tools heat transfer coefficients in semisolid extrusion are primarily affected by the pressure level, in this simulation, the heat transfer coefficients in the stage of solidification and extrusion are taken as 1 and 11 kW/(m²·°C), respectively[15–16]. A friction coefficient of 1.0 at container/billet interface is chosen since the friction coefficient is found to be higher than 0.95 (approximately 1.0) when the temperature of magnesium alloy is above 350 °C[2]. An oil-based graphite lubricant is used at billet/forming die and the friction coefficient is 0.3. Besides the heat exchange between billet and tools, there exist convection and radiation between tools and surrounding environment. The convection coefficient of air is chosen as 0.1 kW/(m²·°C) and the ambient temperature was 20 °C. The lateral surface temperature of the carbon fiber preform measured by thermocouple is chosen as reference value for extrusion temperature.

3 Results and discussion

The simulated result of the temperature distribution in billet during extrusion process at the extrusion temperature of 420 °C is shown in Fig.2. From Fig.2(a), it can be observed that temperature gradient is small along the radial direction of billet at the end of solidification stage. The reason is that the billet is far smaller than tools, and the preheating temperature of

container is higher than that in general hot extrusion. Moreover, the temperature of upper billet is in semisolid zone, and the billet at the exit of forming die has been solidified. Figs.2(b)–(d) indicate that due to the heat exchange between billet and punch as well as heat generation in deformation material in the extrusion stage, the semisolid zone moves gradually toward deformation zone with the punch descending. When the billet in deformation zone is in semisolid state, the small amounts of liquid phase existing on grain boundaries can play a unique role of lubricant. As a result, the grains and fiber in the composite can slip, distort or adjust easily. Thereby, the material has excellent deformability which can be formed utilizing relatively low deforming force. Last but not the least, the liquid phase can feed shrinkage cavities to compact the billet. It can also be noticed that the maximum temperature of billet increases with the extrusion speed increasing. It is well known that the heat generated by the plastic deformation increases and the period for heat dissipation through tooling becomes shorter with the extrusion speed increasing. Accordingly, the temperature of deformation zone increases. If the extrusion speed exceeds the solidification rate of the front edge of semisolid zone, semisolid billet may be extruded out of forming die. And the liquid phase existing at grain boundaries will be oxidized in the atmosphere. Thereby, the grain-boundary strength and

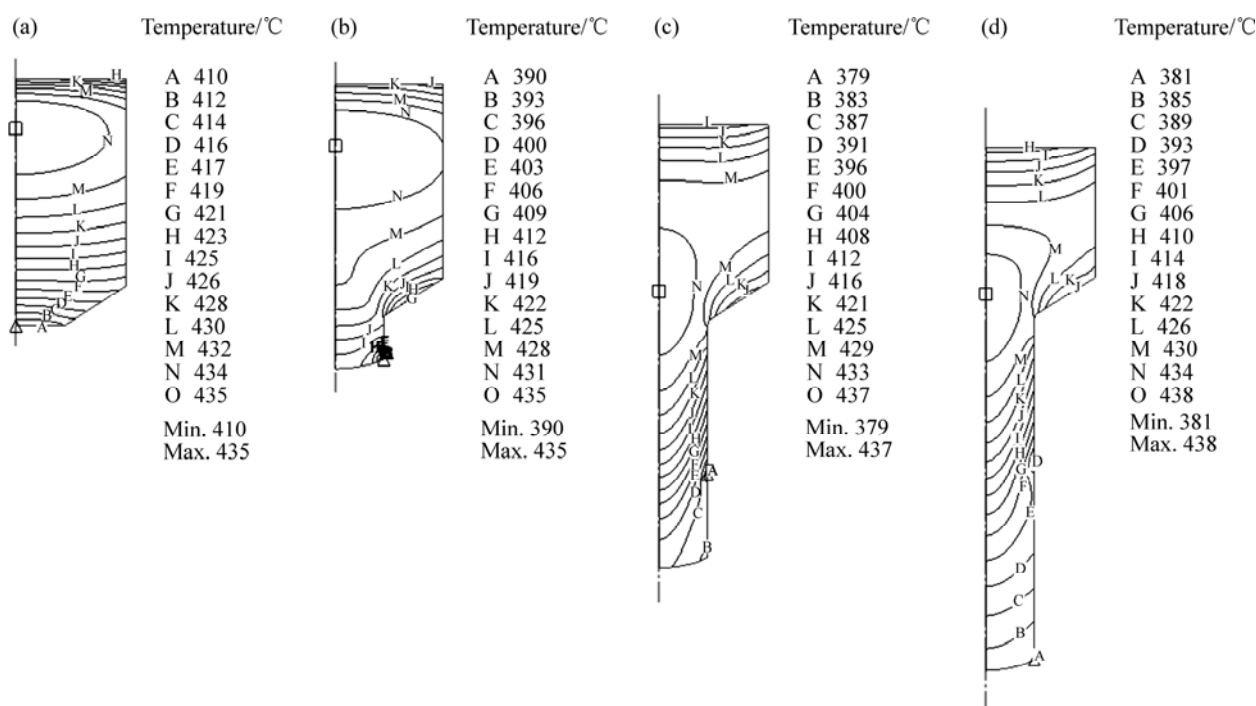


Fig.2 Simulated results of temperature distribution with different punch displacements (extrusion temperature 420 °C, extrusion speed 2.5 mm/s): (a) $D=0$ mm; (b) $D=2$ mm; (c) $D=5$ mm; (d) $D=15$ mm

interfacial strength will be weakened, which will cause the onset of hot shortness cracks.

It was assumed that hot shortness cracks occurred once the surface temperature exceeded the incipient melting temperature. The variation of surface temperature of composite at the exit of forming die is shown in Fig.3. When the extrusion is carried out at extrusion temperature of 420 °C and extrusion speed of 4 mm/s and 2.5 mm/s, the surface temperatures of composite are 430 °C and 427 °C, respectively, which all exceed the incipient melting temperature of composite. However, when the extrusion speed is taken at 1 mm/s, the surface temperature of workpiece is below the incipient melting temperature. So, the critical extrusion

speed is 1 mm/s at extrusion temperature of 420 °C. In the same way, the critical extrusion speed corresponding to different extrusion temperatures can be plotted, as shown in Fig.4. The critical extrusion speeds decrease with increasing the extrusion temperature. When the extrusion temperatures are 390 °C and 420 °C, the critical extrusion speeds allowed are 8 mm/s and 1 mm/s, respectively.

The hot shortness cracks can be avoided according to the established extrusion limit diagram (ELD). However, surface cracks may also occur, even if the process parameters satisfy the established ELD. In this research, Cockcroft & Latham damage model is adopted to predict the onset of surface cracks, and the

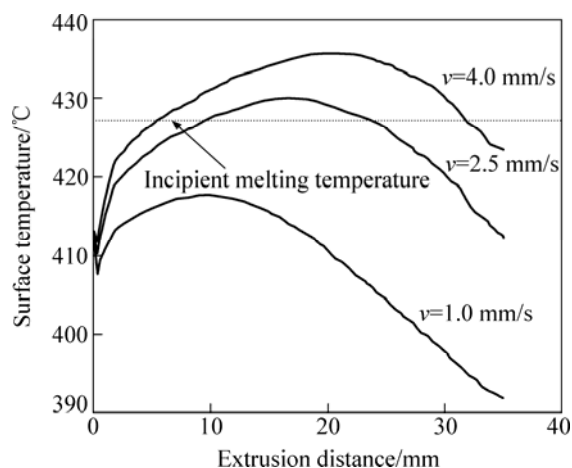


Fig.3 Variation of surface temperature of composite at exit of die (extrusion temperature 420 °C)

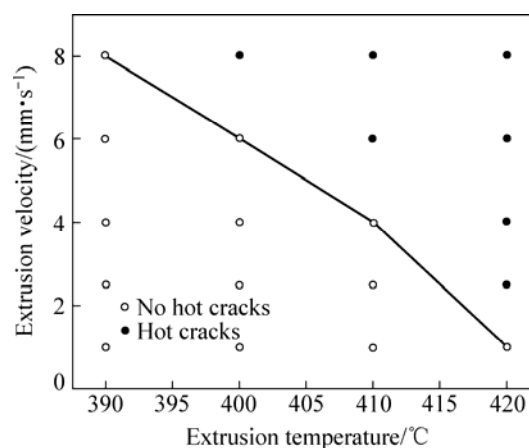


Fig.4 Extrusion limit diagram constructed from FE simulation results

critical damage value C is assumed as 0.45[8]. The maximum damage value of composite as a function of extrusion distance in extrusion temperature range of 400–420 °C and extrusion speed range of 1–6 mm/s is presented in Fig.5. It can be noticed that the curves of the maximum damage fluctuate ranging from 0 to 0.32 when the extrusion speed is 2.4 mm/s or 4 mm/s. However, when the extrusion speed is increased to 6 mm/s, the maximum damage partially exceeds the critical damage value and surface cracks occur. By contrast, when the extrusion temperature is 410 °C and the extrusion speed is either 2.5 mm/s or 4 mm/s, the surface damage value is all below 0.45. When the extrusion temperature is 420 °C and the extrusion speed is 1 mm/s, the maximum damage value range is 0–0.35. Hence, it is not difficult to conclude that the effect of extrusion speed on the surface quality of composite is larger than that of extrusion temperature.

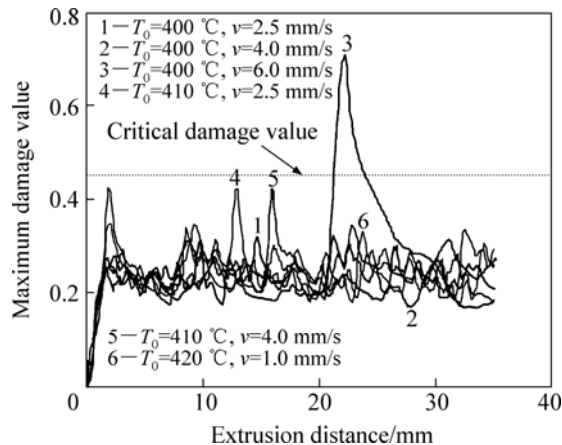


Fig.5 Variations of maximum damage value on surface of composite

In order to validate the reliability of the developed prediction model, the identical process conditions were adopted in the experiments. The composite workpieces the extruded at same extrusion speed and different extrusion temperatures are shown in Fig.6. It can be seen that when extrusion temperature is 400 °C, the maximum damage value is below 0.45, accordingly, the surface quality of composite is sound. When the extrusion temperature is 410 °C and the extrusion speed is the critical value, as shown in Fig.4, the surface damage value is below 0.45, however, it is greater than the former. Correspondingly, there are some slight peelings and no severe cracks on the surface of workpiece. The maximum damage value increases with the extrusion temperature increasing. It can be attributed to the fact that the uneven degree of axial flow rate of composite caused by adhesive friction increases with extrusion temperature increasing. By contrast, when the extrusion temperature is increased to 420 °C, the surface

temperature of composite at the die outlet exceeds the incipient melting temperature. The liquid friction is about 5%, which contributes to the onset of hot shortness. Thereby, the ductility of material deteriorates and severe hot shortness cracks occur under additional tensile stress caused by uneven flow rate. The simulation results agree well with experimental ones.

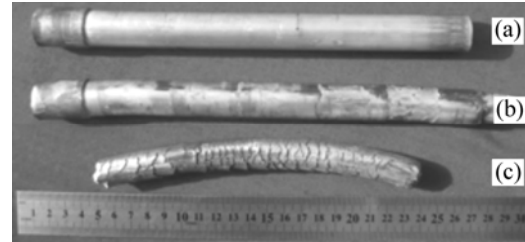


Fig.6 $C_{sf}/AZ91D$ composite workpieces by liquid-solid extrusion ($v=4$ mm/s) at different temperatures: (a) 400 °C; (b) 410 °C; (c) 420 °C

4 Conclusions

1) The critical temperature criterion was used to predict the onset of hot shortness cracks of composite rod by liquid-solid extrusion process, and the extrusion limit diagram for $C_{sf}/AZ91D$ composite was established based on the simulated temperature field. The critical extrusion speeds decrease from 8 mm/s to 1 mm/s as the extrusion temperature increases from 390 °C to 420 °C.

2) The Cockcroft & Latham damage model was used to predict the occurrence of surface cracks of composite formed at the extrusion speed below the critical value based on the established extrusion limit diagram. The maximum damage values increase with the extrusion speed or extrusion temperature increasing.

3) FEM simulation results coincide with those of experiments, which confirms the suitability of the damage prediction method in predicting the onset of hot shortness cracks and surface cracks in the liquid-solid extrusion process.

References

- [1] QI Le-hua, ZHOU Ji-ming, SU Li-zheng, OUYANG Hai-bo, LI He-jun. Fabrication of C_{sf}/Mg composites using extrusion directly following vacuum infiltration—Part 2: Forming process study [J]. Solid State Phenomena, 2008, 141/142/143: 91–96.
- [2] LIU G, ZHOU J, DUSZCZYK J. Prediction and verification of temperature evolution as a function of ram speed during the extrusion of AZ31 alloy into a rectangular section [J]. Journal of Materials Processing Technology, 2007, 186(1/2/3): 191–199.
- [3] LAPOVOK R Y, BAMETT M R, DAVIES C H J. Construction of extrusion limit diagram for AZ31 magnesium alloy by FE simulation [J]. Journal of Materials Processing Technology, 2004, 146(3): 408–414.
- [4] SHIOMI M, TAKANO D, OSAKADA K, OTSU M. Forming of aluminium alloy at temperatures just below melting point [J].

- International Journal of Machine Tools & Manufacture, 2003, 43(3): 229–235.
- [5] FLITTA I, SHEPPARD T. Effect of pressure and temperature variations on FEM prediction of deformation during extrusion [J]. Materials Science and Technology, 2005, 21(3): 339–346.
- [6] HERBA E M, MCQUEEN H J. Influence of particulate reinforcements on 6061 materials in extrusion modeling [J]. Materials Science and Engineering A, 2004, 372(1/2): 1–14.
- [7] OGAWA N, SHIOMI M, OSAKADA K. Forming limit of magnesium alloy at elevated temperatures for precision forging [J]. International Journal of Machine Tools & Manufacture, 2002, 42(5): 607–614.
- [8] HU Hong-jun, ZHANG Ding-fei, PAN Fu-sheng, YANG Ming-bo. Analysis of the cracks formation on surface of extruded magnesium rod based on numerical modeling and experimental verification [J]. Acta Metallurgica Sinica (English Letters), 2009, 22(5): 353–364.
- [9] DUAN X J, VELAY X, SHEPPARD T. Application of finite element method in the hot extrusion of aluminium alloys [J]. Materials Science and Engineering A, 2004, 369(1/2): 66–75.
- [10] ZHANG Xue-min, ZENG Wei-dong, SHU Ying, ZHOU Yi-gang, ZHAO Yong-qing, WU Huan, YU Han-qing. Fracture criterion for predicting surface cracking of Ti40 alloy in hot forming processes [J]. Transactions of Nonferrous Metals Society of China, 2009, 19(2): 267–271.
- [11] WANG Zhen-jun, QI Le-hua, ZHOU Ji-ming. 3D FE analysis on the product defects of composites formed by liquid-solid extrusion process [J]. Journal of Materials Processing Technology, 2009, 209(4): 2068–2076.
- [12] LIU Jian, QI Le-hua, ZHOU Ji-ming, SU Li-zheng. Prediction of surface damage for Al_2O_3 /2A12 composites by liquid infiltration-extrusion process [J]. Chinese Journal of Materials Research, 2009, 23(6): 616–621. (in Chinese)
- [13] SAANOUNI K. On the numerical prediction of the ductile fracture in metal forming [J]. Engineering Fracture Mechanics, 2008, 75: 3545–3559.
- [14] XIONG Shou-mei, XU Qing-yan, KANG Jin-wu. Simulation technology of casting process [M]. Beijing: China Machine Press, 2004. (in Chinese)
- [15] HU H, YU A. Numerical simulation of squeeze cast magnesium alloy AZ91D [J]. Modelling and Simulation in Materials Science and Engineering, 2002, 10(1): 1–11.
- [16] ZHANG Xiao-hua, CHENG Yuan-sheng, LUO Shou-jing. Numerical simulation of temperature field of AZ91D magnesium alloy during equal channel angular extrusion [J]. Acta Metallurgica Sinica (English letters), 2010, 23(1): 35–40.

(Edited by YANG Bing)